

Original Research



Clinical Usefulness of Virtual Ablation Guided Catheter Ablation of Atrial Fibrillation Targeting Restitution Parameter-Guided Catheter Ablation: CUVIA-REGAB Prospective Randomized Study

OPEN ACCESS

Received: Apr 11, 2022

Revised: May 18, 2022

Accepted: Jun 8, 2022

Published online: Jul 11, 2022

Correspondence to

Hui-Nam Pak, MD, PhD

Department of Cardiology, Yonsei University College of Medicine, Yonsei University Health System, 50, Yonsei-ro, Seodaemun-gu, Seoul 03722, Korea.

Email: hnpak@yuhs.ac

Yong-Seog Oh, MD, PhD

Division of Cardiology, Department of Internal Medicine, Seoul St. Mary Hospital, College of Medicine, The Catholic University of Korea, 222, Banpo-daero, Seocho-gu, Seoul 06591, Korea.

Email: oys@catholic.ac.kr

*Young Choi, Byoungyun Lim, Yong-Seog Oh and Hui-Nam Pak have contributed equally to this work and share the first authorship.

Copyright © 2022. The Korean Society of Cardiology

This is an Open Access article distributed under the terms of the Creative Commons Attribution Non-Commercial License (<https://creativecommons.org/licenses/by-nc/4.0>) which permits unrestricted noncommercial use, distribution, and reproduction in any medium, provided the original work is properly cited.

ORCID iDs

Young Choi

<https://orcid.org/0000-0003-3900-1943>

Sung Hwan Kim

<https://orcid.org/0000-0001-6805-0416>

Young Choi , MD, PhD^{1,*}, Byoungyun Lim, PhD^{2,*}, Song-Yi Yang, BSc², So-Hyun Yang, BSc², Oh-Seok Kwon, PhD², Daehoon Kim, MD², Yun Gi Kim, MD, PhD³, Je-Wook Park, MD², Hee Tae Yu, MD, PhD², Tae-Hoon Kim, MD², Pil-Sung Yang, MD⁴, Jae-Sun Uhm, MD, PhD², Jamin Shim, MD, PhD³, Sung Hwan Kim , MD, PhD¹, Jung-Hoon Sung, MD, PhD⁴, Jong-il Choi, MD, PhD³, Boyoung Joung, MD, PhD², Moon-Hyoung Lee, MD, PhD², Young-Hoon Kim, MD, PhD³, Yong-Seog Oh , MD, PhD^{1,*}, Hui-Nam Pak , MD, PhD^{2,*}, and for the CUVIA-REGAB Investigators

¹Division of Cardiology, Department of Internal Medicine, Seoul St. Mary Hospital, College of Medicine, The Catholic University of Korea, Seoul, Korea

²Department of Cardiology, Yonsei University College of Medicine, Yonsei University Health System, Seoul, Korea

³Department of Cardiology, Korea University Cardiovascular Center, Korea University, Seoul, Korea

⁴Department of Cardiology, Bundang CHA Hospital, CHA College of Medicine, Seoul, Korea

AUTHOR'S SUMMARY

Effective ablation approach for persistent atrial fibrillation (PeAF) beyond pulmonary vein (PV) isolation is still controversial. We developed a real-time computational AF modeling technique to perform rapid rotor mapping reflecting the individual electrophysiology and AF mechanisms. In this study, we investigated whether extra-PV ablation targeting a high maximal slope of the action potential duration restitution curve (Smax) improves the outcome of PeAF ablation. However, virtual ablation-guided Smax modulation approach for PeAF did not result in an improved procedural outcome compared to the empirical ablation strategy. Further investigation is needed regarding a more effective patient-customized mechanism-based AF catheter ablation using the functional electrophysiology.


ABSTRACT

Background and Objectives: We investigated whether extra-pulmonary vein (PV) ablation targeting a high maximal slope of the action potential duration restitution curve (Smax) improves the rhythm outcome of persistent atrial fibrillation (PeAF) ablation.

Methods: In this open-label, multi-center, randomized, and controlled trial, 178 PeAF patients were randomized with 1:1 ratio to computational modeling-guided virtual Smax ablation (V-Smax) or empirical ablation (E-ABL) groups. Smax maps were generated by

Yong-Seog Oh 

<https://orcid.org/0000-0003-3567-6505>

Hui-Nam Pak 

<https://orcid.org/0000-0002-3256-3620>

Trial Registration

ClinicalTrials.gov Identifier: [NCT02558699](https://clinicaltrials.gov/ct2/show/study/NCT02558699)

Funding

This work was supported by grants (HI19C0114) and (HI21C0011) from the Ministry of Health and Welfare and grants (NRF-2019R1C1C1009075) and (NRF-2020R1A2B5B01001695) from the Basic Science Research Program run by the National Research Foundation of Korea (NRF), which is funded by the Ministry of Science, ICT & Future Planning (MSIP).

Conflict of Interest

The authors have no financial conflicts of interest.

Data Sharing Statement

The data generated in this study is available from the corresponding authors upon reasonable request.

Author Contributions

Conceptualization: Pak HN; Data curation: Choi Y, Lim B, Yang SY, Kim D, Kim YG, Park JW, Yang PS, Uhm JS, Shim J, Kim SH, Oh YS; Formal analysis: Choi Y, Park JW, Shim J; Funding acquisition: Pak HN; Investigation: Kim TH; Methodology: Lim B, Kim TH; Project administration: Pak HN; Resources: Yang SY, Yang SH, Yu HT, Sung JH, Kim YH; Software: Yang SH, Kwon OS; Supervision: Joung B, Oh YS; Validation: Kwon OS, Lee MH; Visualization: Kim D, Yu HT, Uhm JS, Choi Ji; Writing - original draft: Choi Y, Lim B; Writing - review & editing: Choi Y, Lim B, Pak HN.

computational modeling based on atrial substrate maps acquired during clinical procedures in sinus rhythm. Smax maps were generated during the clinical PV isolation (PVI). The V-Smax group underwent an additional extra-PV ablation after PVI targeting the virtual high Smax sites.

Results: After a mean follow-up period of 12.3±5.2 months, the clinical recurrence rates (25.6% vs. 23.9% in the V-Smax and the E-ABL group, $p=0.880$) or recurrence appearing as atrial tachycardia (11.1% vs. 5.7%, $p=0.169$) did not differ between the 2 groups. The post-ablation cardioversion rate was higher in the V-Smax group than E-ABL group (14.4% vs. 5.7%, $p=0.027$). Among antiarrhythmic drug-free patients ($n=129$), the AF freedom rate was 78.7% in the V-Smax group and 80.9% in the E-ABL group ($p=0.776$). The total procedure time was longer in the V-Smax group ($p=0.008$), but no significant difference was found in the major complication rates ($p=0.497$) between the groups.

Conclusions: Unlike a dominant frequency ablation, the computational modeling-guided V-Smax ablation did not improve the rhythm outcome of the PeAF ablation and had a longer procedure time.

Trial Registration: ClinicalTrials.gov Identifier: [NCT02558699](https://clinicaltrials.gov/ct2/show/study/NCT02558699)

Keywords: Atrial fibrillation; Catheter ablation; Computer simulation; Action potential; Electrophysiology

INTRODUCTION

Atrial fibrillation (AF) is the most common arrhythmia in the world with a higher prevalence in the aging society, and its clinical significance is increasing.¹ AF catheter ablation (AFCA) is the most effective AF rhythm control therapy, which can reduce heart failure mortality, overall deaths or hospitalizations, and the risk of cerebral infarctions or dementia.^{2,3} However, AF is a chronic degenerative disease that exhibits a continuous progression and long-term recurrence even after a one-year successful outcome.⁴ Circumferential pulmonary vein isolation (PVI) is the most crucial and effective ablation target of AFCA.⁵ However, the efficacy of an empirical extra-PV ablation targeting an extra-PV substrate failed to be demonstrated in randomized clinical trials.⁶ AF rotor ablation using basket catheter mapping has a limitation in its low mapping resolution.⁷ Ablation of extra-PV triggers, which are the main mechanism of recurrence after a permanent circumferential PV isolation (CPVI), can improve the rhythm outcome, but the provocation, mapping, and ablation techniques for extra-PV triggers still have limitations.

Recently, on-site realistic human AF modeling that reflects the left atrial (LA) anatomy, histology, and electrophysiology is available during AFCA procedures with an improved computational power.^{8,9} Kim et al.⁸ and Baek et al.¹⁰ reported that a computational modeling-guided AF ablation improves the success rate of a persistent AF (PeAF) ablation as compared to an empirical ablation in the CUVIA-I (118 patients) and II (170 patients) randomized clinical trials. The CUVIA-AF II trial demonstrated an improved PeAF ablation outcome by a computational modeling-guided virtual dominant frequency (DF) ablation.¹⁰ While the DF reflects the high-frequency rotational reentries, a high maximal slope of action potential duration (APD) restitution curve (Smax) indicates a vulnerability to AF wave-brake. The APD restitution is associated with the dynamic heterogeneity of the APD.^{11,12} Thus, a large change in APD with a high Smax makes a circumstance in which a continuous wave-break can be easily sustained.^{13,14} In the APD restitution curve, the

preceding diastolic interval (DI) determines the following APD.¹³⁾¹⁴⁾ A steep (>1) slope of the APD restitution curve means that a small change of the DI causes a large change in the APD. These large APD oscillations make a difference in the refractoriness between adjacent cardiomyocytes, resulting in a local partial conduction block and sustained wave-break from the reentrant wavefront.¹³⁾¹⁴⁾ In this study, we aimed to evaluate the effects of a local extra-PV ablation targeting the high Smax in addition to the CPVI. However, the Smax is a cellular electrophysiology index that is clinically challenging to measure, so we localized the Smax by analyzing the clinical voltage map-integrated AF computational modeling.¹⁴⁾¹⁵⁾ We designed this multi-center prospective randomized clinical trial by collaboration between the clinical ablation team and simulation team in real-time.

In this multi-center randomized clinical trial, the operator acquired an atrial substrate map, sent the data to the modeling team, and received the outcome of the virtual Smax calculated during the CPVI procedure. We compared the rhythm outcomes of the real-time computational modeling-guided extra-PV Smax ablation and empirical AFCA in patients with non-paroxysmal AF.

METHODS

Ethical statement

The Clinical Usefulness of Virtual Ablation Guided Catheter Ablation of Atrial Fibrillation Targeting Restitution Parameter-Guided Catheter Ablation (CUVIA-REGAB) was a multi-center, prospective, single-blind randomized controlled trial including non-valvular AF patients who were scheduled for AFCA (ClinicalTrials.gov number NCT02558699). The study protocol was approved by the Institutional Review Board of each participating center (The Severance Clinical Research Center, IRB No.: 4-2015-0646) and complied with the principles of the 2013 Declaration of Helsinki. All participants provided written informed consent before the study enrollment. The trial enrollment began in March 2019.

Study population

Patients were eligible if they were i) aged 19–80 years and ii) had documented AF despite more than 6 weeks of antiarrhythmic drug (AAD) treatment or documented AF with intolerance to AADs. The major exclusion criteria were an estimated glomerular filtration rate <30 mL/min, contraindication to anticoagulants, cardiac structural abnormalities that were not suitable to a catheter-based AF ablation procedure, history of major bleeding complications, history of a recurrent ischemic stroke, prior AFCA or Maze surgery, or any other conditions that impeded a cardiac computed tomography (CT) scan.

Group assignment and ablation protocol

The included patients were randomly assigned to either the virtual Smax simulation (V-Smax) group or empirical ablation (E-ABL) group in a 1:1 ratio. Randomization was performed by a central randomization service independent of the investigators. All patients received anticoagulation before the AFCA for at least 3 weeks. The AADs were discontinued for at least 5 half-lives prior to the procedure. A cardiac CT scan was performed before the procedure and the absence of any LA appendage thrombus was confirmed. During the ablation procedure, a circular mapping catheter and ablation catheter were advanced into the LA via a transseptal access. Three-dimensional (3D) electroanatomic mapping of the LA was performed in both groups using either an Ensite Navx (Abbott, St. Paul, MN, USA) or CARTO (Biosense Webster,

Diamond Bar, CA, USA) system. In patients with ongoing AF at the beginning of AFCA procedure, intracardiac electrical cardioversion was performed and electroanatomic mapping was conducted during sinus rhythm or regular atrial pacing. If the cardioversion failed or AF recurred during the substrate mapping, a repeated cardioversion was attempted up to 3 times. If AF recurred before the completion of the substrate mapping despite electrical cardioversion, the patient was excluded from the analysis. A CPVI was conducted first in both groups, and the V-Smax group received additional ablation guided by the virtual Smax map (Figure 1). In patients in whom AF remained after the completion of the recommended high Smax site ablation, electrical cardioversion was conducted and the procedure was finished after sinus conversion. In the E-ABL group, further extra-PV ablation was conducted at the operator's discretion. The ablation procedure was performed using radiofrequency energy with an open irrigated catheter with a power of up to 40W. In both groups, ablation of the cavo-tricuspid isthmus line was performed at each operator's discretion.

Computer simulation procedure for an on-site clinical application

The study process in the V-Smax group is shown in Figure 1. At the beginning of the computational modeling procedure, an on-site procedure team acquired the clinical electroanatomical map (voltage map and local activation time [LAT] map) and sent the spatiotemporal data to the core laboratory after integration of the patient's heart CT imaging. The core laboratory team conducted the simulation study using the patient data obtained

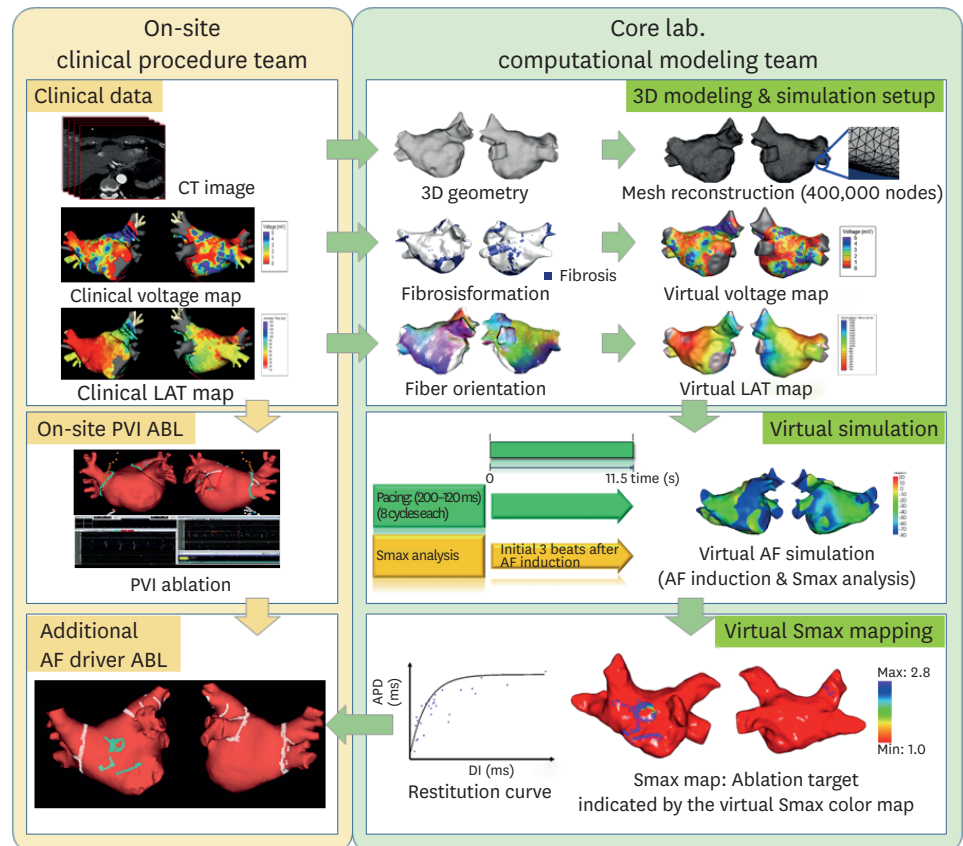


Figure 1. Study process in the V-Smax group. ABL = ablation; AF = atrial fibrillation; CT = computed tomography; LAT = local activation time; PVI = pulmonary vein isolation; 3D = 3-dimensional.

from the procedure team while the on-site operators started the CPVI. Merging of the LAT and voltage maps with the CT images were performed by 4 steps: geometry, trimming, field scaling, and alignment.¹⁶⁾ The clinical electroanatomical map merged with CT was created to obtain the clinical LAT and voltage maps. We acquired the clinical voltage map that was recorded on the LA during sinus rhythm or regular atrial pacing based on bipolar electrograms. We merged the 3D LA modeling results with CT images of the patient's heart and then adjusted them with the clinical map.

3D computational modeling of AF and virtual Smax mapping

The detailed description of the 3D computational modeling is provided in the supplemental methods. The LA geometries were reconstructed from the 3D CT digital images and communication in medicine files.⁹⁾ The virtual LAT and voltage map of the LA were generated and synchronized with the clinical maps using the CUVIA software (Model: SH01; Laonmed Inc., Seoul, Korea). To determine the Smax for each node, the APD of 90% (APD₉₀) and DI were measured during ramp pacing for the duration from the start of the pacing to 3 beats after AF induction. Then the APD restitution curve was determined by employing the relationship between the APD₉₀ and DI, and the Smax was calculated via the maximal slope of the restitution curve, defined at each node of the LA model. The generated Smax map was transmitted to the on-site procedure team for the V-Smax ablation. The region with the highest 10% Smax value was provided by a color-coded Smax map which was normalized between the minimum and maximum V-Smax values of overall nodes for each patient in the V-Smax group. Mean Smax value was 1.00 ± 0.33 . We ablated the highest 10% Smax area to minimize the critical mass reduction effects.

Follow up and outcome analysis

The primary study endpoint was a freedom from any atrial tachyarrhythmia recurrence for 12 months. The secondary study endpoints were periprocedural mortality, major bleeding, thromboembolic complications, then procedure time, and total ablation time. Major bleeding was defined as a cardiac tamponade requiring intervention or bleeding events that required a transfusion or resulted in more than a 4 g/dL decrease in the hemoglobin. Post-procedural AADs were used at each operator's discretion for 3 months after the AFCA, then the AADs were discontinued when there was no recurrent AF. Patients were routinely scheduled to visit our outpatient clinic at 1, 3, 6, and 12 months after the AFCA and every 6 months thereafter. A 12-lead electrocardiogram (ECG) was recorded on every visit, and 24-hour Holter monitoring was performed at 3, 6, and 12 months. After a 3-month blanking period, any AF or atrial tachycardia (AT) recorded on the 12-lead ECG or lasting for more than 30 seconds on the Holter testing was considered a recurrence. All clinical outcomes of interest were confirmed and adjudicated by the central clinical events committee.

Statistical analysis

The sample size was estimated from the recurrence rate derived from the CUVIA-I trial.⁸⁾ The AF recurrence rates were presumed to be 20% in the Smax simulation group and 40% in the empirical ablation group. An overall sample size of more than 172 was expected to have an 80% power to detect a statistical difference between the 2 groups at a 2-sided alpha of 0.05. For the baseline characteristics, the continuous variables are presented as the mean \pm standard deviation and were compared using Student's t-tests. Categorical variables are presented as frequencies with percentages (%) and were compared by the χ^2 test or Fisher's exact test. The cumulative incidence of the primary outcome was estimated by Kaplan-Meier survival curves and compared with the log-rank test. In the overall population, a multivariate Cox

proportional hazard regression analysis was used to adjust the risk of the outcome of interest and to identify independent predictors. All variables with p values <0.2 in the univariate Cox regression analysis and other non-significant variables with a proven importance to predict AF recurrence were included in a multivariate Cox proportional hazards regression model. For all 2-tailed comparison, p values <0.05 were considered to indicate statistical significance. All the statistical analyses were performed using SPSS version 25.0 software (SPSS Inc., Chicago, IL, USA).

RESULTS

Baseline characteristics

Among a total of 196 patients with AAD-resistant symptomatic PeAF undergoing catheter ablation, 18 (9.2%) were excluded due to a failed internal cardioversion or 3 episodes of recurrent AF re-initiated during paced atrial substrate mapping, which provided the mandatory electrophysiologic data for our realistic computation modeling (**Figure 2**). A total of 178 patients were included in the study, including 90 allocated to the V-Smax group and 88 to the E-ABL group. The mean age was 62.2 ± 9.9 years and 131 (73.6%) were male (**Table 1**). The median AF duration was 31 (15–66) months and the mean CHA₂DS₂-Vasc score was 2.2 ± 1.3 . The mean LA dimension (antero-posterior diameter) was 43.0 ± 6.1 mm, and the left ventricular ejection fraction was $56.6 \pm 8.7\%$. Both groups were well-balanced, and there was no significant difference in the baseline characteristics between the 2 groups.

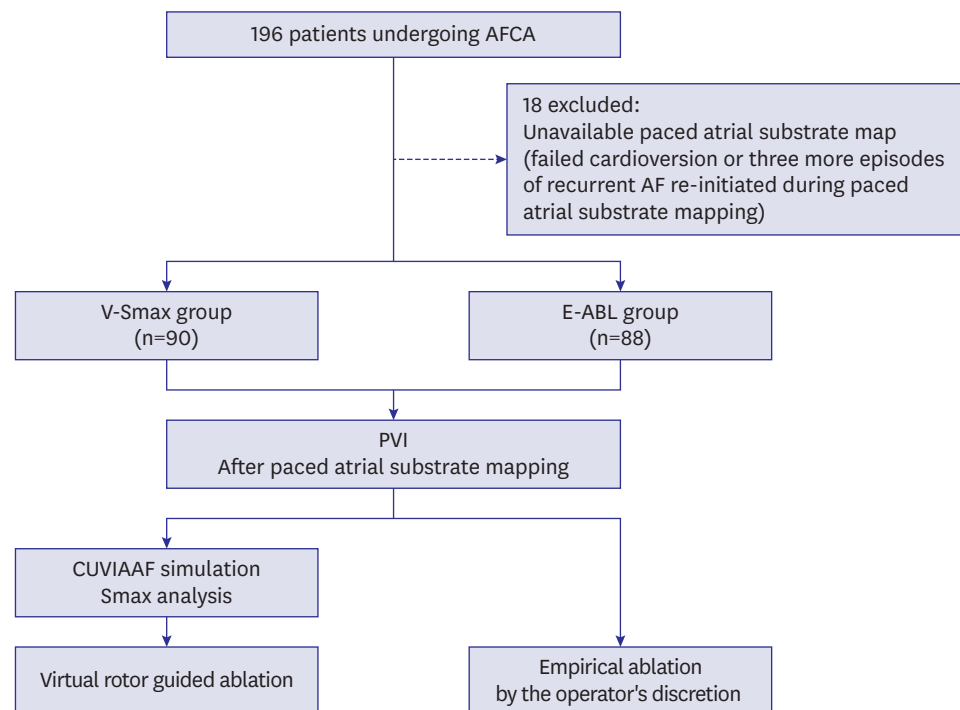


Figure 2. Study enrollment. Included patients were randomly assigned to receive virtual rotor guided ablation or empirical ablation therapy.

AF = atrial fibrillation; AFCA = atrial fibrillation catheter ablation; E-ABL = empirical ablation; PVI = pulmonary vein isolation; V-Smax = virtual high maximal slope of the action potential duration restitution curve simulation.

Table 1. Baseline clinical characteristics

Characteristics	Overall (n=178)	V-Smax (n=90)	E-ABL (n=88)	p value
Age, years	62.2±9.9	62.9±9.6	61.3±10.1	0.279
Male	131 (73.6)	66 (73.3)	65 (73.9)	0.936
AF duration (months; n=169)	49.5±47.6	48.9±45.6	50.0±49.9	0.878
AF duration, median (IQR)	31 (15–66)	30 (12–72)	34 (17–64)	-
Comorbidities				
Heart failure	47 (26.4)	28 (31.1)	19 (21.6)	0.150
Hypertension	128 (71.9)	67 (74.4)	61 (69.3)	0.447
Diabetes mellitus	40 (22.5)	24 (26.7)	16 (18.2)	0.175
Stroke	9 (5.1)	4 (4.4)	5 (5.7)	0.745
Vascular disease	14 (7.9)	9 (10.0)	5 (5.7)	0.285
CHA ₂ DS ₂ -VASC score	2.2±1.3	2.3±1.4	2.1±1.3	0.221
Echocardiographic parameters				
LA dimension (mm; n=172)	43.0±6.1	43.4±6.1	42.6±6.1	0.376
LA volume index (mL/m ² ; n=114)	40.1±16.7	41.6±16.5	38.6±16.8	0.331
LV ejection fraction (%; n=178)	56.6±8.7	56.2±8.7	57.0±8.7	0.514
E/Em (n=160)	9.4±3.3	9.5±3.3	9.2±3.4	0.529
LVEDD (mm; n=178)	48.7±5.6	48.8±5.7	48.7±5.4	0.839
LVMI (n=168)	97.7±28.6	97.3±27.8	98.2±29.6	0.838
Smax value (n=147)	1.00±0.33	1.04±0.32	0.96±0.34	0.108

Values are presented as mean±standard deviation or number (%).

AF = atrial fibrillation; E-ABL = empirical ablation; E/Em = mitral inflow velocity/mitral annulus tissue velocity; IQR = interquartile range; LA = left atrial; LV = left ventricle; LVEDD = left ventricle end-diastolic diameter; LVMI = left ventricle mass index; PeAF = persistent atrial fibrillation; Smax = high maximal slope of the action potential duration restitution curve; V-Smax = virtual Smax simulation.

Table 2. Procedure related characteristics

Characteristics	Overall (n=178)	V-Smax (n=90)	E-ABL (n=88)	p value
Procedure time (minutes; n=174)	194.6±52.3	205.2±56.5	184.2±45.8	0.008
Ablation time (seconds; n=168)	3,353.4±1,228.3	3,610.7±1,334.6	3,083.6±1,047.7	0.005
Ablation lesions (%)				
CPVI	178 (100)	90 (100)	88 (100)	-
CTI	159 (89.3)	81 (90.0)	78 (88.6)	0.768
Smax ablations				
Roof		33 (36.7)		
Anterior wall		37 (41.1)		
Septum		37 (41.1)		
Posterior inferior wall		26 (28.9)		
Left lateral isthmus area		21 (23.3)		
Linear Ablations (%; BDB rates)				
Roof line			21 (23.9, 66.7)	
Posterior box ablation			7 (8.0, 71.4)	
Anterior line			16 (18.2, 75.0)	
Septal line			5 (5.7, 0)	
CFAE ablation			15 (17.0, 0)	
Complications	13 (7.3)	6 (6.7)	3 (3.4)	0.498
Tamponade	6	4	2	-
Pneumonia	1	0	1	-
Sick sinus syndrome	1	1	0	-
Tachy brady syndrome	1	1	0	-

BDB = bidirectional block; CFAE = complex fractionated atrial electrogram; CPVI = circumferential pulmonary vein isolation; CTI = cavotricuspid isthmus; E-ABL = empirical ablation; V-Smax = virtual high maximal slope of the action potential duration restitution curve simulation.

Procedural characteristics

The CPVI was completed in all patients and additional cavo-tricuspid isthmus ablation was performed in 159 (89.3%) patients (**Table 2**). The mean Smax values were 1.04±0.32 in the V-Smax group and 0.96±0.34 in the E-ABL group (p=0.108). The Smax for the E-ABL was calculated by a post hoc analysis. The high Smax area was located within the low voltage area in 93.5% of the patients and corresponded to the slow conduction zone in 72.3% of the

patients. Among the total of 522 high Smax sites, 58.2% were in the areas of disorganized fiber orientation (septum, appendage base, roof of coronary sinus, or PV antrum). In the V-Smax group, additional extra-PV ablation targeting Smax sites was conducted on the roof area (36.7%), anterior wall (41.1%), antero-septum (41.1%), posterior wall (28.9%), and left lateral isthmus area (23.3%), respectively (Table 2, Supplementary Figure 1). In the E-ABL group, extra-PV ablation was conducted for roof line in 23.9%, anterior line in 18.2%, septal line in 5.7%, and posterior box in 8.0% of patients. The bidirectional block rates of the linear ablation were 66.7%, 75.0%, and 71.4% for the roof line, anterior line, and posterior box isolation, respectively. The total procedure time was significantly longer in the V-Smax group than E-ABL group (p=0.008). The major complication rates did not significantly differ between the 2 groups (p=0.498, Table 2). There were 4 cases of intraprocedural cardiac tamponade requiring emergent pericardiocentesis in the V-Smax group. Three of them were developed during CPVI, and the other one was developed during cavo-tricuspid isthmus ablation performed for previously documented atrial flutter. None of the cardiac tamponades were associated with virtual high Smax sites ablation, and all patients were fully recovered.

Procedure outcomes

The mean follow-up duration was 12.3± 5.2 months. After the AFCA, AADs were prescribed in 49 patients (27.5%) after 3 months and 84 (47.2%) patients at the final follow-up, without a significant difference between the 2 groups (Table 3). Recurrence of atrial arrhythmias after the blanking period was observed in 23 (25.6%) patients in the V-Smax group and 21 (23.9%) in the empirical ablation group (log rank, p=0.880) (Figure 3A). According to the mode of recurrence, AT recurrences among the overall clinical recurrences were 43.5% in the V-Smax group and 23.8% in the E-ABL group (p=0.169, Table 3). However, the post-AFCA cardioversion rate was significantly higher in the V-Smax group (14.4%) than E-ABL group (5.7%, p=0.027). In patients who were not prescribed any AAD after 3 months, the AF freedom rate was 52/66 (78.7%) in the V-Smax group and 51/63 (80.9%) in the E-ABL group (p=0.776, Figure 3B). In the multivariate analysis, only AF duration and LA volume index were independent predictors for a clinical recurrence (Table 4). The computational modeling-guided Smax ablation was not associated with higher AF freedom. In a sub-group analysis according to the global average of Smax value, the rhythm outcome did not differ between the patients with an Smax ≥1.0 and those with an Smax <1.0 in either the V-Smax group (Log-rank p=0.796) or E-ABL group (p=0.504) (Figure 4A and B). Examples of Smax maps that represent patients with high (≥1) and low (<1) Smax values are shown in Figure 4C and D.

Table 3. Clinical rhythm outcomes

Characteristics	Overall (n=178)	V-Smax (n=90)	E-ABL (n=88)	p value
Follow-up duration (months)	12.3±5.2	12.3±5.1	12.2±5.4	0.848
Post-ABL medication				
ACEi or ARB	103 (58.5)	59 (66.3)	44 (50.6)	0.034
Beta blocker	78 (44.3)	39 (43.8)	39 (44.8)	0.893
Statin	83 (47.2)	45 (50.6)	38 (43.7)	0.360
AAD use				
AADs at discharge	99 (55.6)	50 (55.6)	49 (55.7)	0.986
AADs after 3 months	49 (27.5)	24 (26.7)	25 (28.4)	0.795
AADs at the final follow-up	84 (47.2)	47 (52.2)	37 (42.0)	0.174
Early recurrence	41 (23.0)	24 (26.7)	17 (19.3)	0.244
Clinical recurrence	44 (24.7)	23 (25.6)	21 (23.9)	0.794
Recurrence as AT, n (% in recur/% overall)	15 (34.1)	10 (43.5/11.1)	5 (23.8/5.7)	0.169
Cardioversion, n (% in recur/% overall)	18 (40.9/10.1)	13 (56.5/14.4)	5 (23.8/5.7)	0.027

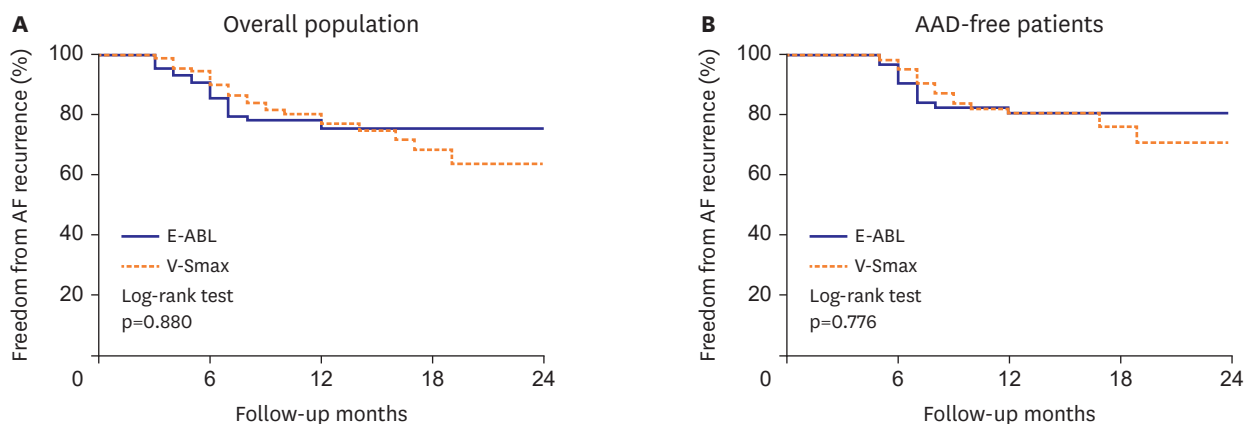
AAD = antiarrhythmic drug; ABL = ablation; ACEi = angiotensin-converting enzyme inhibitor; ARB = angiotensin receptor blocker; AT = atrial tachycardia; E-ABL = empirical ablation; V-Smax = virtual high maximal slope of the action potential duration restitution curve simulation.

Table 4. Cox regression analysis for clinical recurrence

Characteristics	Univariate		Multivariate*	
	HR (95% CI)	p value	HR (95% CI)	p value
Age (years)	1.00 (0.97–1.03)	0.745	0.99 (0.94–1.04)	0.649
Male	0.52 (0.28–0.94)	0.031	0.73 (0.30–1.77)	0.486
AF duration	1.01 (1.00–1.01)	0.070	1.01 (1.00–1.02)	0.003
Comorbidities				
Heart failure	0.76 (0.38–1.54)	0.446	0.66 (0.22–1.95)	0.449
Hypertension	0.77 (0.41–1.44)	0.408		
Diabetes mellitus	0.90 (0.43–1.87)	0.780		
Stroke	1.64 (0.58–4.58)	0.349		
Vascular disease	0.76 (0.24–2.47)	0.651		
CHA ₂ DS ₂ -VASc score	1.01 (0.81–1.26)	0.954		
Echocardiographic parameters				
LA dimension (mm)	1.04 (0.99–1.10)	0.134		
LA volume index (mL/m ²)	1.02 (1.00–1.04)	0.045	1.02 (1.00–1.05)	0.047
LV ejection fraction (%)	1.04 (0.99–1.08)	0.111		
E/Em	1.04 (0.95–1.13)	0.442		
LVEDD (mm)	0.96 (0.90–1.02)	0.163		
LVMi (g/m ²)	1.00 (0.98–1.01)	0.443		
Smax simulation	1.05 (0.58–1.89)	0.881	1.38 (0.62–3.06)	0.421

AF = atrial fibrillation; CI = confidence interval; E/Em = mitral inflow velocity/mitral annulus tissue velocity; HR = hazard ratio; LA = left atrial; LV = left ventricle; LVEDD = left ventricle end-diastolic diameter; LVMi = left ventricle mass index.

*Among the variables with p values <0.2 in univariate analyses, LA dimension, LV ejection fraction, and LVEDD were excluded in the multivariate analysis to avoid multicollinearity.



Numbers at risk					
E-ABL	88	73	38	12	0
V-Smax	90	76	38	14	0

Numbers at risk					
E-ABL	63	62	41	19	0
V-Smax	66	64	43	18	0

Figure 3. Freedom from AF recurrence in the 2 groups. (A) AF freedom in overall patients. (B) AF freedom in AAD-free patients at 3 months after AFCA. AAD = antiarrhythmic drug; AF = atrial fibrillation; AFCA = atrial fibrillation catheter ablation; E-ABL = empirical ablation; V-Smax = virtual high maximal slope of the action potential duration restitution curve simulation.

DISCUSSION

This multicenter prospective randomized clinical trial evaluated the efficacy of the on-site computational modeling-guided Smax ablation approach in patients with PeAF. Unlike a DF ablation, the V-Smax ablation in addition to the CPVI did not improve the procedure outcomes as compared to an empirical PeAF ablation and rather increased the total procedure time. The on-site application of the realistic computational modeling of AF, which reflects a personalized atrial anatomy, electrophysiology, fibrosis, and fiber orientation, is feasible, but the Smax may not be an appropriate extra-PV ablation target in patients with non-paroxysmal AF.

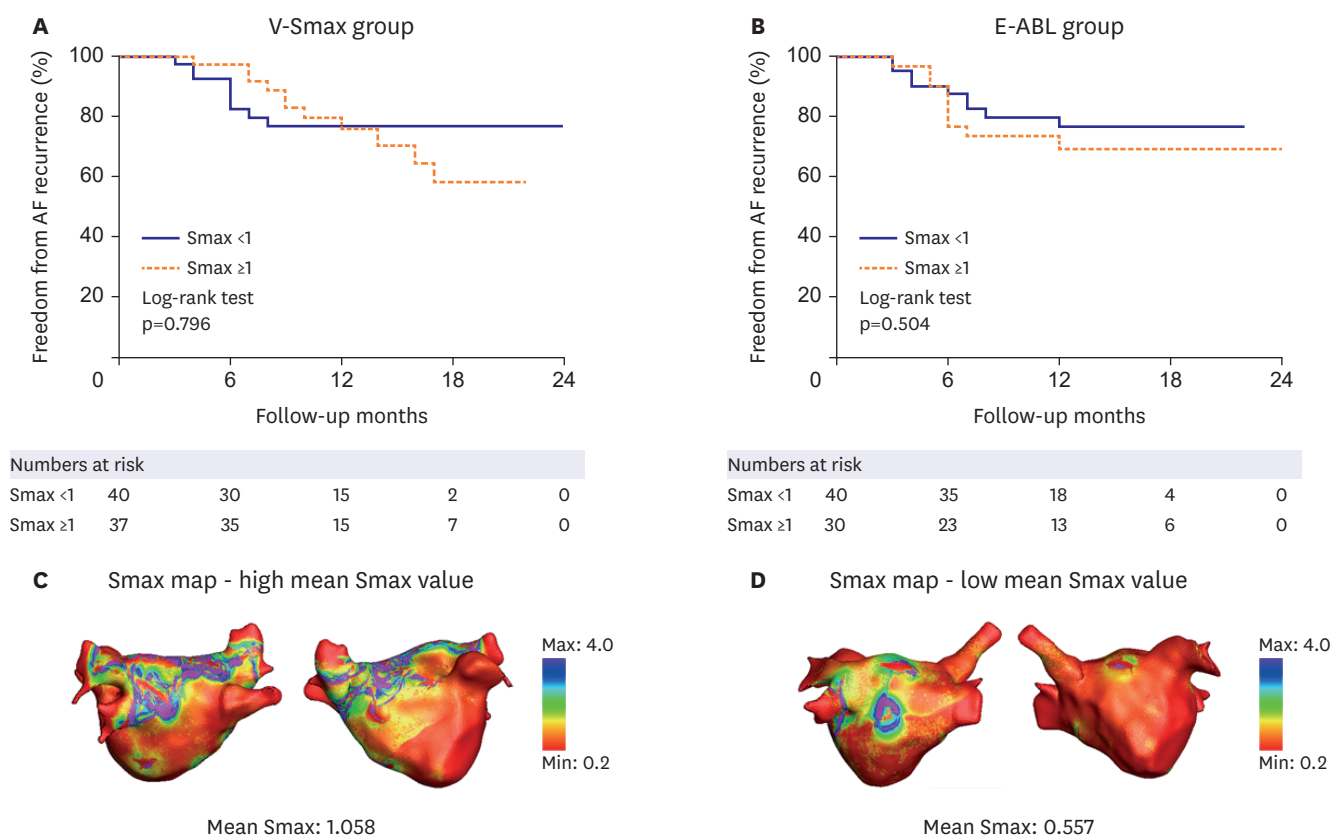


Figure 4. Subgroup analysis according to the Smax level. (A) Freedom from AF in patients with Smax <1 and Smax ≥1 in the V-Smax group. (B) Freedom from AF in patients with Smax <1 and Smax ≥1 in the E-ABL group. Representative virtual Smax maps in patients with high Smax (C) and low Smax (D) values. AF = atrial fibrillation; E-ABL = empirical ablation; V-Smax = virtual high maximal slope of the action potential duration restitution curve simulation.

It has already been confirmed that the CPVI is the most effective target for AFCA, but little is known about its proper extra-PV targets. In the case of non-paroxysmal AF with advanced atrial remodeling, the amount and location of a substrate change varies from patient to patient. Because of these personalized characteristics, all randomized clinical trials that tested for a uniform empirical additional extra-PV ablation beyond the CPVI failed to demonstrate their efficacy.⁴⁾⁶⁾ Since then, a late gadolinium enhancement (LGE) on magnetic resonance imaging (MRI), low voltage area mapping, or catheter mapping of AF drivers by a multi-electrode catheter have been attempted to apply tailored approaches that reflect the patient characteristics.¹⁷⁾ However, in the case of an MRI-LGE or low voltage area ablation, the electrophysiological properties of AF were not reflected.¹⁸⁾ Roving multi-electrode catheter AF mapping has a limitation in that it is not a synchronized entire chamber AF map, and focal impulse and rotor mapping have a limitation of the low spatial resolution of the basket catheter.

To overcome these problems, we devised a computational modeling-guided AF map.⁸⁾⁹⁾ We tried to find the proper ablation target in the induced virtual AF after integrating the CT-based anatomical information, personalized atrial voltage, and activation information acquired at the beginning of the AFCA procedure into the human AF modeling.¹⁶⁾ Since the CUVIA AF modeling is an entire chamber map including the histological information such as fibrosis and the myocardial fiber orientation, it is possible to determine the precise extra-PV ablation target with AF wave dynamics parameters together at more than 400,000 sophisticated nodes.⁹⁾ The virtual AF map analyzed with the mapping data acquired at the

beginning of the procedure can be calculated within about 30–40 minutes of the operator performing CPVI, enabling on-site simulation tests.¹⁰⁾ In this study, the Smax, an index representing the AF wave break vulnerability, was extracted by computational modeling and applied to clinical procedures.¹⁹⁾

In general, the Smax is an indicator of the wave break vulnerability, and the DF represents a focal source or focal driver in AF maintenance mechanisms.¹⁵⁾ In the CUVIA AF II study, extra-PV DF ablation improved the rhythm outcome of the PeAF ablation,¹⁰⁾ but the V-Smax ablation did not affect the ablation outcome in this study. However, it is difficult to assert that the focal source mechanism is the primary mechanism of the AF maintenance rather than a continuous wave break. That is because the degree of meandering of the AF driver changes according to the cellular and tissue electrophysiological conditions of the atrium, and the 2 mechanisms are interchangeable.²⁰⁾ Hwang et al.²¹⁾ reported an inverse relationship between the Smax and DF, and Park et al.²²⁾ reported that a DF ablation improved the rhythm outcome only in the low Smax patient group in the CUVIA AF2 post hoc analyses. In other words, it means that there is an interaction between the Smax and DF. However, unlike the localized DF sites, the distribution of the Smax was very heterogeneous, making it difficult to target, and it prolonged the procedure time. The V-Smax group had a prolonged procedure time owing to a diffuse ablation time.

It has been 25 years since the procedure called AFCA first started, and the outcome is improving, but it still has a significant long-term recurrence rate.⁴⁾ Various empirical, histology-based, and rotor tracing extra-PV ablation methods have been tried to reduce the postoperative recurrence in PeAF patients, but none of them have been sufficient to improve the rhythm outcome.^{4,6)} Therefore, it can be expected that the AFCA results will be improved by additionally reflecting the personalized electrophysiologic character of AF. Recently, by utilizing computational modeling, it has become possible to perform procedures considering the electrophysiology and AF mechanisms, as well as the anatomy and histology. Hwang et al.²¹⁾ compared and evaluated the virtual ablation of the DF, phase singularity, Shannon's entropy, and complex fractionated atrial electrograms, and showed that the DF ablation had the most effective anti-AF effects, which were also shown in clinical studies.¹⁰⁾ In this study, the effect of the Smax ablation reflecting the dynamic heterogeneity of the refractoriness was clinically evaluated. The Smax ablation had an AF defragmentation effect but did not improve the clinical rhythm outcomes. In the future, a more effective patient-customized mechanism-based AFCA using the functional electrophysiology will improve the sophisticated AF mapping and procedural outcomes.

There are several limitations to our study. First, there was no constant protocol for the empirical ablation strategy. There might have been a significant between-center difference in the ablation protocol and procedural outcomes in the E-ABL group. The Smax ablation was performed based on the anatomic area recommended by the computation model, which was not precisely matched in the 3-dimensional electroanatomic maps. The use of AADs after the AFCA was not strictly regulated without any statistical differences between the groups. Because we performed cardioversion to acquire the substrate map, we could not evaluate the AF termination rate during the Smax ablation. Smax could depend on the computational model used. Electrotonic effects, caused by variations in the geometry and fibrosis, may affect Smax but may not be precisely reflected in this personalized modeling. We selected the ablation target by an empirical cutoff of highest 10% Smax area, which was chosen empirically. Although it is not demonstrated in our study, Smax ablation could be potentially proarrhythmic by providing

stable anchoring sites for reentrant drivers. The recurrence rate in the E-ABL group was lower (23.9%) than expected (40%) at study designation. Thus the study might not have been adequately powered to detect the efficacy of the virtual simulation guided ablation strategy.

In conclusion, in this multi-center prospective randomized trial, computational AF modeling and virtual ablation targeting a restitution parameter-guided Smax ablation in addition to the CPVI was not associated with an improved arrhythmia freedom expensing longer procedure time than an empirical ablation strategy in patients with PeAF.

ACKNOWLEDGMENTS

We would like to thank Mr. John Martin for his linguistic assistance.

SUPPLEMENTARY MATERIALS

Supplementary Data 1

Methods

[Click here to view](#)

Supplementary Figure 1

(A) The frequencies of Smax ablation sites in V-Smax group. (B) Frequency of empirical extra-pulmonary vein linear ablation sites in E-ABL group.

[Click here to view](#)

Supplementary References

[Click here to view](#)

REFERENCES

1. Kannel WB, Abbott RD, Savage DD, McNamara PM. Epidemiologic features of chronic atrial fibrillation: the Framingham study. *N Engl J Med* 1982;306:1018-22.
[PUBMED](#) | [CROSSREF](#)
2. Packer DL, Mark DB, Robb RA, et al. Effect of catheter ablation vs antiarrhythmic drug therapy on mortality, stroke, bleeding, and cardiac arrest among patients with atrial fibrillation: the CABANA randomized clinical trial. *JAMA* 2019;321:1261-74.
[PUBMED](#) | [CROSSREF](#)
3. Kim D, Yang PS, Sung JH, et al. Less dementia after catheter ablation for atrial fibrillation: a nationwide cohort study. *Eur Heart J* 2020;41:4483-93.
[PUBMED](#) | [CROSSREF](#)
4. Verma A, Jiang CY, Betts TR, et al. Approaches to catheter ablation for persistent atrial fibrillation. *N Engl J Med* 2015;372:1812-22.
[PUBMED](#) | [CROSSREF](#)
5. Pak HN, Park JW, Yang SY, et al. Cryoballoon versus high-power, short-duration radiofrequency ablation for pulmonary vein isolation in patients with paroxysmal atrial fibrillation: a single-center, prospective, randomized study. *Circ Arrhythm Electrophysiol* 2021;14:e010040.
[PUBMED](#) | [CROSSREF](#)

6. Lee JM, Shim J, Park J, et al. The electrical isolation of the left atrial posterior wall in catheter ablation of persistent atrial fibrillation. *JACC Clin Electrophysiol* 2019;5:1253-61.
[PUBMED](#) | [CROSSREF](#)
7. Narayan SM, Krummen DE, Shivkumar K, Clopton P, Rappel WJ, Miller JM. Treatment of atrial fibrillation by the ablation of localized sources: CONFIRM (Conventional Ablation for Atrial Fibrillation With or Without Focal Impulse and Rotor Modulation) trial. *J Am Coll Cardiol* 2012;60:628-36.
[PUBMED](#) | [CROSSREF](#)
8. Kim IS, Lim B, Shim J, et al. Clinical usefulness of computational modeling-guided persistent atrial fibrillation ablation: updated outcome of multicenter randomized study. *Front Physiol* 2019;10:1512.
[PUBMED](#) | [CROSSREF](#)
9. Shim J, Hwang M, Song JS, et al. Virtual *in-silico* modeling guided catheter ablation predicts effective linear ablation lesion set for longstanding persistent atrial fibrillation: multicenter prospective randomized study. *Front Physiol* 2017;8:792.
[PUBMED](#) | [CROSSREF](#)
10. Baek YS, Kwon OS, Lim B, et al. Clinical outcomes of computational virtual mapping-guided catheter ablation in patients with persistent atrial fibrillation: a multicenter prospective randomized clinical trial. *Front Cardiovasc Med* 2021;8:772665.
[PUBMED](#) | [CROSSREF](#)
11. Krummen DE, Bayer JD, Ho J, et al. Mechanisms of human atrial fibrillation initiation: clinical and computational studies of repolarization restitution and activation latency. *Circ Arrhythm Electrophysiol* 2012;5:1149-59.
[PUBMED](#) | [CROSSREF](#)
12. Narayan SM, Kazi D, Krummen DE, Rappel WJ. Repolarization and activation restitution near human pulmonary veins and atrial fibrillation initiation: a mechanism for the initiation of atrial fibrillation by premature beats. *J Am Coll Cardiol* 2008;52:1222-30.
[PUBMED](#) | [CROSSREF](#)
13. Qu Z, Weiss JN, Garfinkel A. Cardiac electrical restitution properties and stability of reentrant spiral waves: a simulation study. *Am J Physiol* 1999;276:H269-83.
[PUBMED](#) | [CROSSREF](#)
14. Weiss JN, Garfinkel A, Karagueuzian HS, Qu Z, Chen PS. Chaos and the transition to ventricular fibrillation: a new approach to antiarrhythmic drug evaluation. *Circulation* 1999;99:2819-26.
[PUBMED](#) | [CROSSREF](#)
15. Kim BS, Kim YH, Hwang GS, et al. Action potential duration restitution kinetics in human atrial fibrillation. *J Am Coll Cardiol* 2002;39:1329-36.
[PUBMED](#) | [CROSSREF](#)
16. Lim B, Kim J, Hwang M, et al. In situ procedure for high-efficiency computational modeling of atrial fibrillation reflecting personal anatomy, fiber orientation, fibrosis, and electrophysiology. *Sci Rep* 2020;10:2417.
[PUBMED](#) | [CROSSREF](#)
17. Kim TH, Uhm JS, Kim JY, Joung B, Lee MH, Pak HN. Does additional electrogram-guided ablation after linear ablation reduce recurrence after catheter ablation for longstanding persistent atrial fibrillation? A prospective randomized study. *J Am Heart Assoc* 2017;6:6.
[PUBMED](#) | [CROSSREF](#)
18. Marrouche NF, Wilber D, Hindricks G, et al. Association of atrial tissue fibrosis identified by delayed enhancement MRI and atrial fibrillation catheter ablation: the DECAAF study. *JAMA* 2014;311:498-506.
[PUBMED](#) | [CROSSREF](#)
19. Lim B, Hwang M, Song JS, et al. Effectiveness of atrial fibrillation rotor ablation is dependent on conduction velocity: an in-silico 3-dimensional modeling study. *PLoS One* 2017;12:e0190398.
[PUBMED](#) | [CROSSREF](#)
20. Li C, Lim B, Hwang M, et al. The spatiotemporal stability of dominant frequency sites in in-silico modeling of 3-dimensional left atrial mapping of atrial fibrillation. *PLoS One* 2016;11:e0160017.
[PUBMED](#) | [CROSSREF](#)
21. Hwang I, Park JW, Kwon OS, et al. Spatial changes in the atrial fibrillation wave-dynamics after using antiarrhythmic drugs: a computational modeling study. *Front Physiol* 2021;12:733543.
[PUBMED](#) | [CROSSREF](#)
22. Park JW, Lim B, Hwang I, et al. Restitution slope affects the outcome of dominant frequency ablation in persistent atrial fibrillation: CUVIA-AF2 post-hoc analysis based on computational modeling study. *Front Cardiovasc Med* 2022;9:838646.
[PUBMED](#) | [CROSSREF](#)